JOURNAL OF MATERIALS SCIENCE 17 (1982) 2309–2323

The thermal expansion of particulate-reinforced composites

S. J. FELTHAM*, B. YATES
Department of Pure and Applied Physics, University of Salford, Salford, UK

R. J. MARTIN
Plastics Division, Ciba-Geigy Plastics and Additives Company, Duxford, Cambridge, UK

After describing the development and standardization of interferometric apparatus employed to measure linear thermal expansion coefficients of materials over the approximate temperature range 80 K to 310 K, an account of an investigation of particulate reinforced Ciba-Geigy epoxy resin CY219/HY219/DY219 is given. The successful conclusion of an appraisal of schemes attempting to describe the dependence of the thermal expansion characteristics of a composite upon the volume-fraction of its filler was followed by a search for particle-size effects. No such effects were observed in composites reinforced with silica flour, glass microspheres and copper powder.

Nomenclature

$\beta_m, \beta_i, \beta_c$	volume thermal expansion coeffients of the matrix, inclusions and composite, respectively.
E_m, E_i, E_c	Young's moduli of the matrix, inclusions and composite, respectively.
K_m, K_i, K_c	bulk moduli of the matrix, inclusions and composite, respectively.
n_m, n_i, n_c	rigidity moduli of the matrix, inclusions and composite, respectively.
ν_m, ν_i, ν_c	Poisson's ratios of the matrix, inclusions and composite, respectively.
V_m, V_i	volume-fractions of matrix and inclusions, respectively.

1. Introduction

Particulate-reinforced epoxy resins possess a variety of attractive physical properties. An appropriate choice of fillers can lead to the production of mechanically and thermally stable composites possessing good adhesion characteristics, which may be cast or moulded to achieve faithful reproductions of fine detail. Other attributes include good thermal and electrical resistance, as well as the ability to resist chemical attack. The last characteristics hold particular attractions for the encapsulation of electrical components which require protection from the environment.

The efficient utilization of composites in applications such as these requires the controlled adjustment of the thermal expansion characteristics to match those of the components being encapsulated. This is the background against which the present investigation was undertaken, to examine the detailed influence of the size and volume-fraction of the inclusions upon the thermal expansion characteristics of reinforced resins. In order to enhance the value of the results, the temperature range of the investigation was extended from ambient to cover the approximate range 80 K to 310 K.

2. The specimens

2.1. Constituent materials

All the composites studied were based upon the same matrix resin system, Ciba-Geigy 219. Fillers used at different stages were:

(a) silica flour, supplied by Hoben Davis Ltd, Newcastle-under-Lyme;

*Present address: Thorn EMI Varian, Hayes, Middlesex, UK.

0022–2461/82/082309–15$04.30/0

(b) solid glass microspheres supplied by Potters–Ballotini Ltd, Barnsley, the composition of a typical sample of which is given in Table I; and

(c) copper powder, supplied by Powder Metallurgy Ltd, London.

2.2. Preparation

In order to ensure that surface moisture was completely removed from the inclusion materials before being incorporated in samples, these were heated to a temperature of 373 K in a fan oven, where they remained for 48 h before specimen preparation commenced. The matrix was prepared by weighing the constituents, resin CY219, hardener HY219 and accelerator DY219, into a beaker in the proportions 100, 50 and 2 parts, by weight, respectively. When composites were being prepared, the appropriate quantity of inclusion material was added and the mixture was thoroughly stirred to ensure complete wetting of the filler particles. To avoid sedimentation of the filler in the low-viscosity matrix resin during cure, and to effect de-aeration, the mixture was then subjected to an "advancement" step by stirring continuously for about 80 min at 323 K under vacuum in a water bath, or until the limit of pourability was approached. The resin was then transferred to the mould, which had been pre-heated to a temperature of 373 K in the oven, where the curing was allowed to proceed over the following 24 h. The effectiveness of the mixing process was subsequently confirmed by cutting a thin slice from the composite and examining this under a microscope, when the particle distribution was found to be uniformly random, displaying no evidence of sedimentation. The specimen of pure resin was produced in a similar manner, except that no inclusions were added.

Specimens in two forms, tubes and rods, were employed, all of which were approximately 10 mm long. The tubes were produced to internal and external diameters 20 mm and 28 mm, respectively, and the rods took the form of prisms with triangular cross-sections. A diamond-impregnated rotary disc saw, lubricated by Aquigrinde 80 solution, was employed in specimen preparation, all stages of which were performed slowly in order to ensure that the thermal and mechanical properties of the specimen were not influenced by local heating effects.

TABLE I Typical composition of soda-lime glass from which microspheres are manufactured

Constituent	Composition (%)
SiO_2	72.8
CaO	8.5
MgO	3.4
Na_2O	12.5
K_2O	1.0
Al_2O_3	1.7
Fe_2O_3	0.1

TABLE II Designations of specimens containing silica flour

Particle diameter range (μm)	Inclusion volume-fraction (%)			
	10	20	30	40
45–53		5		
53–63	1	2	3	4
63–75		6		
105–125		7		

Complete summaries of the specimens employed in the investigation are collected in Tables II and III, in which a specimen of fused glass microspheres was included. Sieves were employed to separate the particles into groups classified according to the size ranges given in Tables II and III.

3. Experimental details

3.1. The apparatus

3.1.1. The specimen chamber

The original form taken by the apparatus employed to execute the present programme was described by Waterhouse and Yates [1]. It has been improved by subsequent users over the years, for example, [2, 3], and it is appropriate that the form taken by it at the conclusion of the present investigation should be recorded.

The specimen chamber is shown schematically in Fig. 1. It may be considered to consist of three sections. The window section, Section A, was designed to permit easy replacement of the specimen chamber window. The assembly consisted of a truncated copper cone, D, soldered into a sealing flange, F_1. The specimen chamber window, G, was made from a silica glass plate, polished flat to within $\lambda/5$. It was held in position inside D by Araldite type AT1 compound. F_1 mated with a flange, F_2, located on the main specimen chamber body, B. F_1 and F_2 were treated with Loctite Stud Lock and secured together with six screws to form a high-vacuum seal, E. To ensure stray reflections were thrown out of the field of view,

TABLE III Designations of supplementary specimens

Specimen number	Description of specimen	Particle diameter range (μm)
8	Pure resin	
9	Fused glass microspheres	
10	Resin containing glass microspheres ($V_i = 20\%$)	0–44
11	Resin containing glass microspheres ($V_i = 20\%$)	177–297
12	Resin containing copper powder ($V_i = 20\%$)	0–44
13	Resin containing copper powder ($V_i = 20\%$)	177–297

F_1 was machined at an angle such that when Section A was positioned onto Section B, the window was off-set at a small angle from the horizontal.

Section B comprised the main body of the specimen chamber. The lower portion, from flange K_1 downwards, was machined to produce two supporting limbs. The base was formed by a copper plate, Q, which was screwed onto the support limbs and which bore three screws, U. These screws provided kinematic support for the interferometer stand, R. Inside R was the interferometer assembly, consisting of the lower and upper optically flat plates, T_1 and T_2, and the specimen(s).

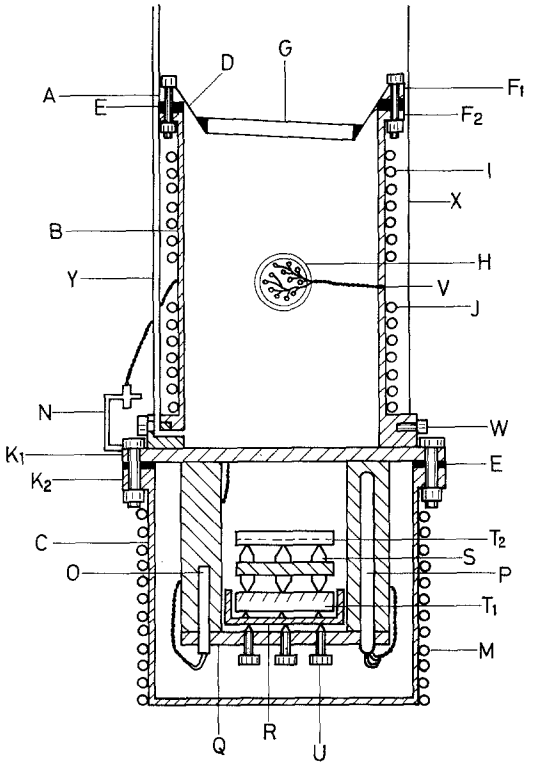

Figure 1 The specimen chamber. A, window section; B, main body section; C, interferometer cover section; D, truncated copper cone; E, Loctite seal; F_1, F_2, flanges; G, silica glass window; H, pin seal; I, J, heater elements; K_1, K_2, flanges; M, heater element; N, tag strip; O, platinum sensor; P, platinum thermometer; Q, base plate; R, interferometer stand; S, specimens; T_1, T_2, lower and upper optically flat plates; U, levelling screws; V, wire core; W, specimen chamber support screw; X, cryostat support tube; Y, pumping tube.

A wire core, V, entered the chamber through a pin seal, H, soldered into the chamber wall. The wall also supported two non-inductively wound heater elements, I and J. I was wound above the pin seal, while J occupied the area below H. In addition, a third heater element, M, was wound around Section C. Both the wiring core and heater elements were protected and thermally anchored to the specimen chamber with low-temperature varnish, GE7031.

Section C, comprising the interferometer cover, was manufactured from copper. The function of this section was to seal the specimen chamber while maintaining easy access to the interferometer assembly. This was achieved by clamping flanges K_1 and K_2 with eight screws and using Loctite Stud Lock as a vacuum gasket.

The temperature control of the specimen chamber was achieved with the aid of a temperature controller designed by Gluyas and Harwood [4], actuated by a commercial platinum resistance sensor, O, to maintain the temperature constant to better than 0.02 K during a period of 1 h, over the range 77 K to 373 K. The temperature was measured with a 4-lead platinum resistance thermometer, P, supplied by H. Tinsley and Co. Ltd, and calibrated by the National Physical Laboratory.

3.1.2. The optical system

The optical system is shown schematically in Fig. 2. The source of illumination was a helium–neon laser, LS, operating at a wavelength, λ, of 632.8 nm. The laser was fitted with a collimating lens and a spatial filter. The width of the collimated beam was adjusted so that it just covered the interferometer plates and its intensity distribution was spatially uniform.

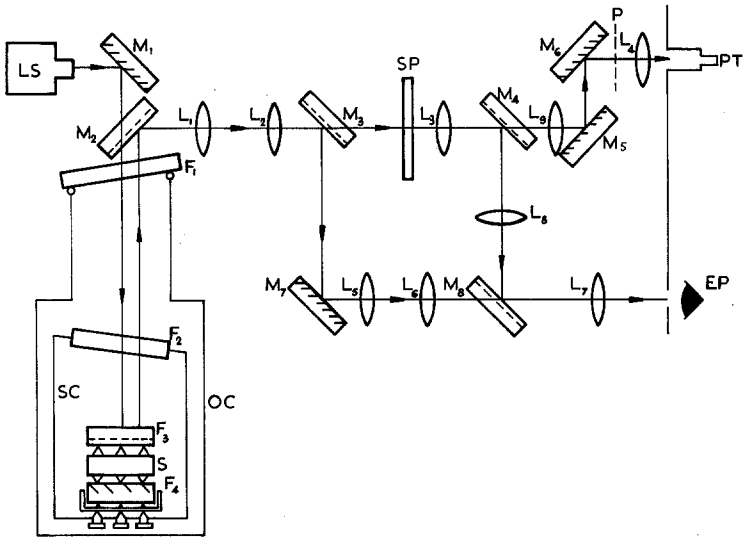

Figure 2 The optical system. LS, laser; M_1, M_5, M_6, M_7, fully aluminized mirrors; M_2, M_3, M_4, M_8, partially aluminized mirrors; L_1 to L_9, converging lenses; SP, slit plate; P, Polaroid filter; F_1, cryostat window; F_2, specimen chamber window; F_3, F_4, interferometer plates; S, specimen; SC, specimen chamber; OC, outer can; EP, eye-piece; PT, photomultiplier tube.

The beam entered the cryostat via M_1, F_1 and F_2, where F_1 and F_2 were optically flat silica glass plates and M_1 was a fully reflecting plane mirror. (All mirrors and plates used in the optical system were polished flat to within $\lambda/5$ unless otherwise stated.) F_1 rested on a lightly greased "O"-ring which formed the vacuum seal between the cryostat and the light-tight box, housing the optical detection system. As explained earlier, F_2 was permanently fixed in position by Araldite type AT1, and formed a window between the specimen chamber and the outer can. Both F_1 and F_2 were off-set by a small angle from the horizontal in order to prevent spurious reflections from interfering with the main image.

The interferometer consisted of two silica glass plates F_3 and F_4, diameter 30 mm and thickness 5 mm, flat to within $\lambda/20$. The upper surface of F_4 was fully aluminized. The lower surface of F_3 was partially aluminized, while its upper surface contained a fully aluminized rectangular area which formed part of the fiduciary system. In addition, this surface was cut at an angle of about 40′ arc to its bottom surface, to throw unwanted reflections out of the field of view. The two plates were separated by the specimen, S, which was set such that an optical wedge was formed. Within the optical wedge, reflected light interfered with the incident light, thus producing an interference pattern. Interfering rays were then returned along their original path, towards M_2. At M_2 the light was reflected towards M_3. M_3 was a partially aluminized mirror which divided the beam into two branches. The first, called the setting beam, was focused onto an eye-piece. The second branch, called the slit-plate beam, was focused onto a plate, SP, which contained three slits. The slit-plate beam was split into two sub-branches by M_4. One sub-branch recombined with the setting beam at the mirror M_8. Both the sub-branch and the setting beam were made to follow similar optical path lengths and thus when viewed with the eye-piece they appeared superimposed. The other sub-branch, the intensity of which was controlled by means of crossed polaroids, P, was focused onto a photomultiplier tube, PT. P was rotated about the beam axis until the galvanometer monitoring the photomultiplier output indicated a full-scale deflection.

The interferometer was located within the specimen chamber, as shown in Fig. 1. The other components of the optical system were mounted inside a light-tight box, which was blackened on the inside in order to prevent stray reflections from interfering with the operation of the apparatus.

As explained earlier, specimens took the form of either a single hollow tube or a set of three rods. In the latter case, the rods, which had pointed ends, were supported in a vertical attitude within a brass specimen holder. In the former case three small feet were ground on each end of the tubular specimen. The specimen lengths were adjusted until the angle between the interferometer plates was correct for the production of four interference fringes in the field of view.

3.2. Experimental procedure

A rise in specimen temperature caused a movement of interference fringes in a direction perpendicular to their length and this formed the basis of the

experimental method for the determination of the linear thermal expansion coefficient of the specimen(s) separating the interferometer plates. The purpose of the slit plate, SP (see Fig. 2), was two-fold. Reference to Fig. 3a will show that this contained two reference slits, at right-angles to one another, and a slit through which light from the interference fringes might pass. The upper face of plate, F_3 (see Fig. 2), bore a fully aluminized region bounded by two black strips of tape, as shown in Fig. 3b. In order to ensure that fringe movement observations were always made with respect to a fixed fiduciary system, coupled movements of the x- and y-slits were effected by means of a cable-drive mechanism until, with the aid of the photomultiplier, the alignment depicted in Fig. 3c was achieved. The fringe slit (Fig. 3a) was next rotated until it was parallel to the interference fringes, following which the pressure of helium exchange gas between the interferometer plates was adjusted until the photomultiplier gave a reading corresponding to the mid-point of the steeper side of one of the (asymmetric) fringes. Raising the temperature by a measured amount, typically 10 K, caused a movement of fringes which was registered by a chart recorder. After checking the alignment of the reference slits with respect to the fiduciary system, the pressure of the exchange gas within the specimen chamber was adjusted in a controlled manner until the photomultiplier galvanometer gave a reading corresponding to the mid-point of the steeper side of a fringe. The linear thermal expansion coefficient of the specimen(s), of height, h, was then calculated from

$$\alpha = \frac{1}{(T_2 - T_1)}\left[\frac{F\lambda}{2h} + K\left(\frac{p_1}{T_1} - \frac{p_2}{T_2}\right)\right], \quad (1)$$

where p_1 and p_2 are the initial and final pressures of exchange gas at temperatures T_1 and T_2, F is the integral movement of interference fringes of wavelength, λ, and K is the constant in the equation of Gladstone and Dale [5],

$$K = \frac{T}{p}(\mu - 1), \quad (2)$$

where μ is the refractive index of the exchange gas at temperature, T, and pressure, p.

An assessment of the precision and accuracy of which the system is capable was made by measuring the linear thermal expansion coefficient of specimens of standard fused silica, SRM739, obtained from the National Bureau of Standards (NBS). In order to effect a fair assessment of the capabilities of the apparatus, the same specimen holder was employed for the NBS specimens as was used to support the composite rod specimens during the main investigation. The results are compared with those of Kirby and Hahn [6] in Fig. 4. The different sets of results agree within the limits of experimental uncertainty at all temperatures.

4. Results

The results of the main part of the investigation are displayed in Figs 5 and 6. It will be seen later that an appraisal of these results led to investigations of the thermal-expansion characteristics of specimens of resin reinforced with glass microspheres and copper powder, the results of which are displayed in Figs 7 and 8. In order to be able to understand the results in quantitative terms, the thermal expansion characteristics of specimens of pure resin and fused glass microspheres were also investigated, the results of which are displayed in Figs 9 and 10.

5. Discussion

Although the main aim of the present study was to investigate the influence of the volume-fraction and particulate size of the inclusions upon the thermal-expansion characteristics of resin-contain-

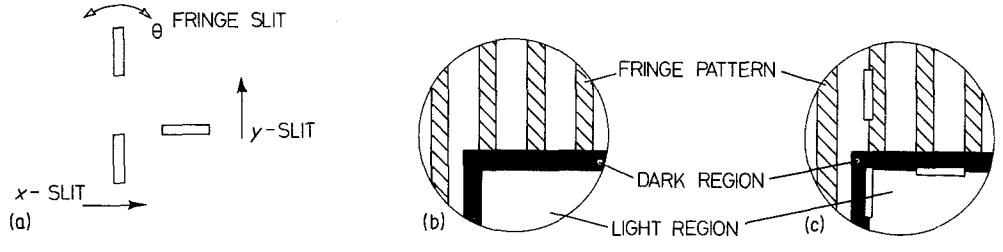

Figure 3 The interferometer field of view and associated slit system: (a) the slit system, (b) the fiduciary system and fringes and (c) alignment of slits with fiduciary system.

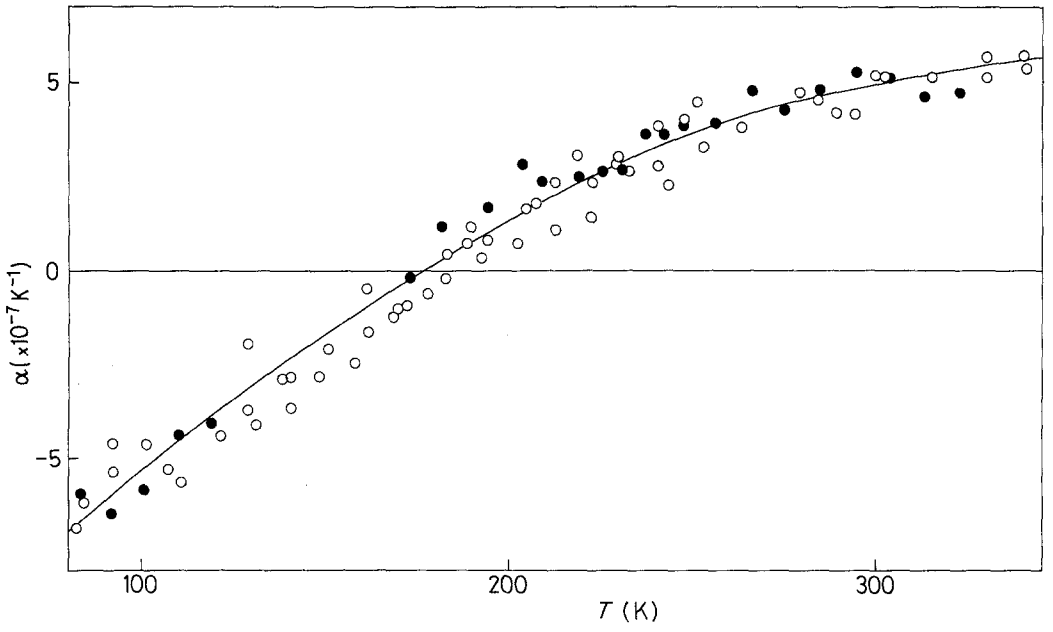

Figure 4 The linear thermal expansion coefficient, α, of fused silica (SRM 739 from the National Bureau of Standards). Present primary data: ○, using original specimen chamber; ●, using new specimen chamber. Solid line, smoothed NBS data [6].

ing fillers, the thermal-expansion characteristics of the constituents of the composites contained interest in their own right.

5.1. Composite constituents

5.1.1. Pure resin CY219/HY219/DY219

The specimens of pure resin took the form of a set of three rods. Runs 1 and 2 of the results, which are displayed in Fig. 9, were undertaken using the specimen chamber described earlier [1–3], whereas Run 3 was undertaken some 22 months later, with the aid of the new specimen chamber. Since the capabilities of the two specimen chambers to reproduce standarized NBS results for fused silica had been established, the agreement between the results of runs undertaken at widely differing times might be taken to indicate the absence of any detectable influence of ageing or moisture absorption in the thermal-expansion characteristics of the unreinforced resin.

This observation should be qualified by explaining that the specimen chamber was pumped for 24 h before the commencement of measurements, in order to remove any surface moisture which might have contaminated the helium exchange gas, affected the refractive index and led to erroneous calculations. One cannot say whether or not this precautionary treatment had removed moisture which had penetrated to a significant depth in the specimens, which were in the chamber at the time.

A note of caution might be issued in making this observation. Earlier observations of the temperature dependences of the linear thermal expansion coefficients of epoxy resins failed to show up effects resulting from suspected molecular re-arrangements, which became manifest when the thermal expansion of the resin matrix was restrained by the presence of unidirectionally reinforcing fibres [8, 9]. A parallel situation may exist in the case of moisture absorption, i.e., it is possible that moisture in a resin produces internal changes which only manifest themselves in the thermal expansion characteristics when the resin is mechanically stressed. Until more is known about these effects the results are probably best taken at their face value.

Examination of Fig. 9 reveals that while the linear thermal expansion coefficients of the epoxy resins ERLA 4617/mPDA, DLS351/$BF_3$400 and Code 69 are very similar to one another over the temperature range covered, the results for the resin CY219/HY219/DY219 stand distinctly higher. This difference may be attributed to the substantially lower cross-link density in the latter product.

5.1.2. Fused glass microspheres

In order to be able to measure the linear thermal

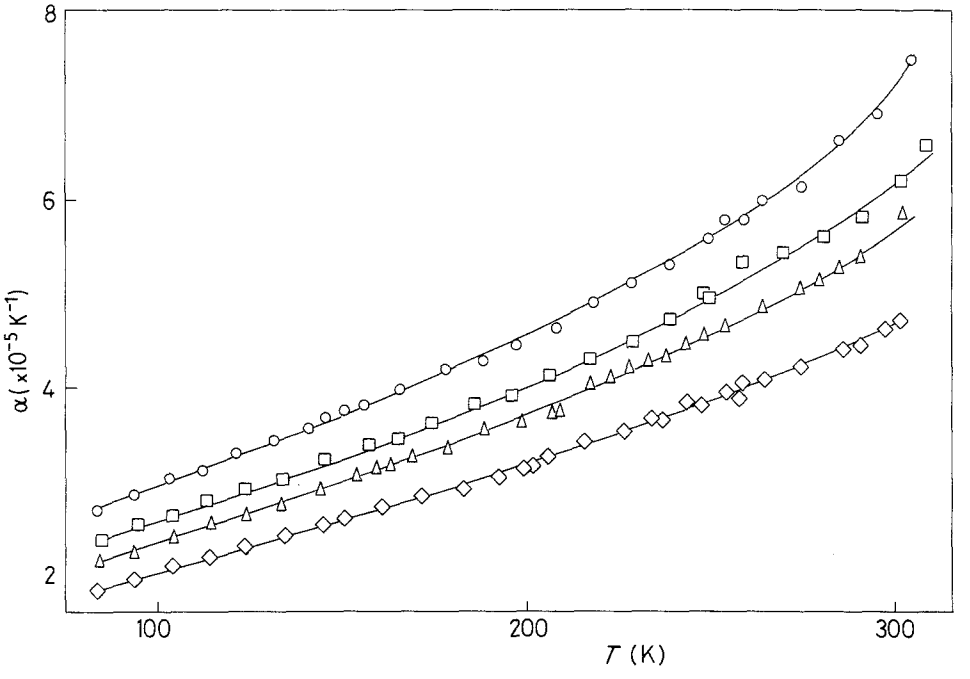

Figure 5 The influence of inclusion volume-fraction, V_i, upon the linear thermal expansion coefficient, α, of Ciba-Geigy epoxy resin, CY219/HY219/DY219, containing silica flour having a mean particle diameter of 58 μm: ○, Specimen 1 ($V_i = 10\%$); □, Specimen 2 ($V_i = 20\%$); △, Specimen 3 ($V_i = 30\%$); and ◇, Specimen 4 ($V_i = 40\%$).

expansion coefficient of the glass microspheres, a quantity of these were fused together to form a single hollow cylindrical specimen. The results for this specimen are displayed in Fig. 10.

Perhaps the most distinctive feature of the linear thermal expansion coefficients of glasses is their generally small magnitude, which frequently assumes negative values over extensive ranges of low temperature. An explanation of a contribution to negative expansion in terms of transverse

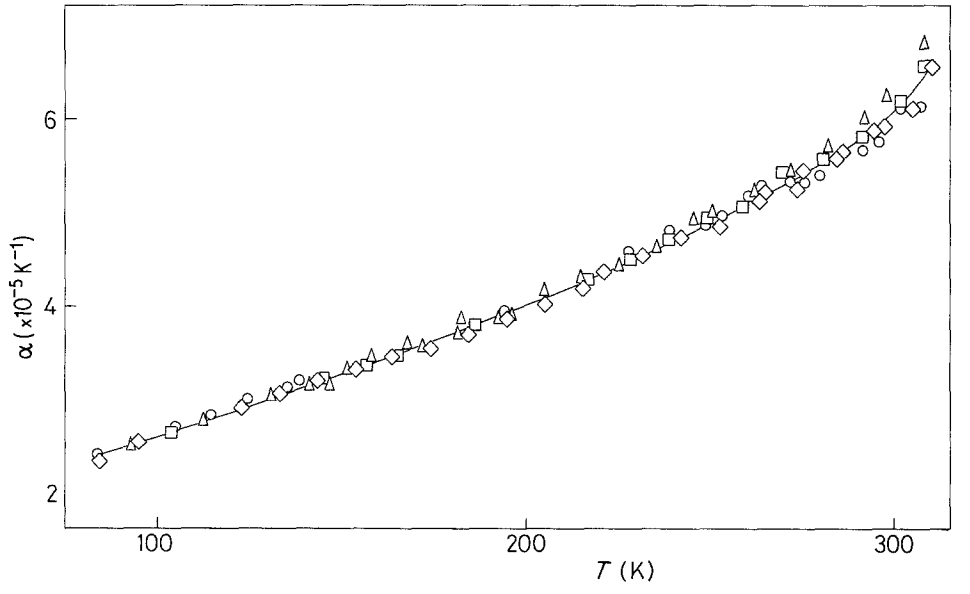

Figure 6 The influence of inclusion mean diameter, d_i, upon the linear thermal expansion coefficient, α, of Ciba-Geigy epoxy resin CY219/HY219/DY219 containing silica flour at a nominal volume-fraction of 20%: ○, Specimen 5 ($d_i = 49\,\mu$m); □, Specimen 2 ($d_i = 58\,\mu$m); △, Specimen 6 ($d_i = 69\,\mu$m); and ◇, Specimen 7 ($d_i = 115\,\mu$m).

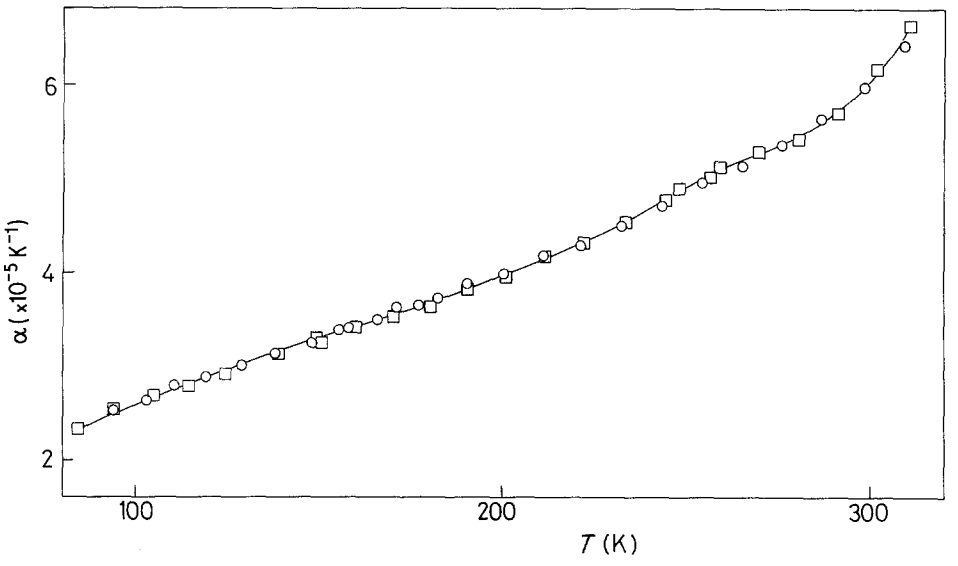

Figure 7 The influence of inclusion mean diameter, d_i, upon the linear thermal expansion coefficient, α, of Ciba-Geigy epoxy resin CY219/HY219/DY219 containing solid glass microspheres at a nominal volume-fraction of 20%: ○, Specimen 10 ($d_i = 22\,\mu m$); and □, Specimen 11 ($d_i = 237\,\mu m$).

vibrations of the atoms of vitreous and other forms of silica was provided by Smyth [10], who showed that these structures caused the frequencies of such vibrations to decrease as the structures themselves shrank. Barron [11] and Blackman [12] arrived at similar results and the conclusions that negative expansion coefficients were to be expected from open structures rather than close-packed ones, and that those with relatively low shear moduli would be favoured, has been substantiated on a number of subsequent occasions, for example, [13]. In fact, the thermal expansion of the present glass was larger than many, indicating only a small contribution from the transverse modes of vibration compared with that from the longitudinal modes. The reason for this was presumably the combined high concentrations of sodium and calcium (see Table I), which act as network modifiers and inhibit transverse vibrations of constituent oxygen atoms. The

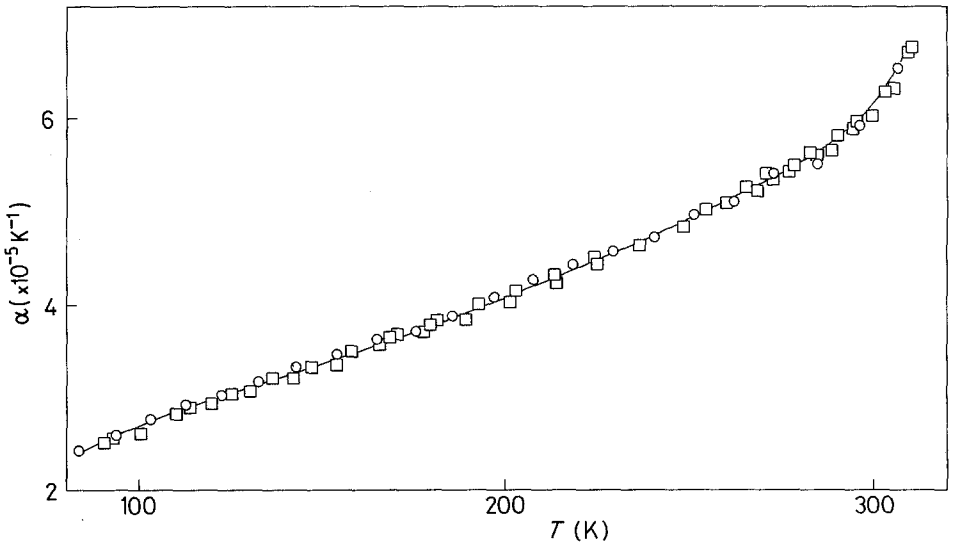

Figure 8 The influence of inclusion mean diameter, d_i, upon the linear thermal expansion coefficient, α of Ciba-Geigy epoxy resin CY219/HY219/DY219 containing copper powder at a nominal volume-fraction of 20%: ○, Specimen 12 ($d_i = 22\,\mu m$); and □, Specimen 13 ($d_i = 237\,\mu m$).

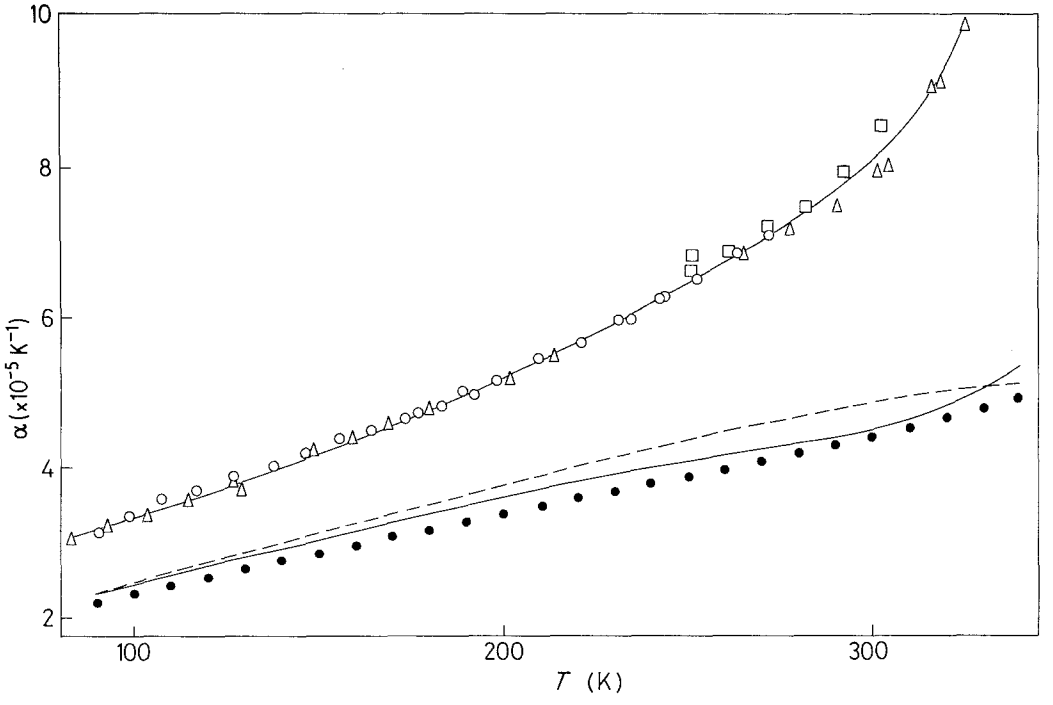

Figure 9 Comparison of smoothed primary data for the linear thermal expansion coefficient, α, of resin system, CY219/HY219/DY219, with smoothed results for other epoxy resin systems: CY219/HY219/DY219: ○ Run 1, □ Run 2, △ Run 3; ——— ERLA4617/mPDA [7]; — — — DLS351/$BF_3$400 [8]; · · · · · · · Code 69 [9].

composition of this specimen was very similar tc that of the sample of soda-lime glass, Number 0081 from Corning Glass Works, New York, included in the study undertaken by White [14]. The Corning Glass Company quote a linear thermal expansion coefficient of $9 \times 10^{-6}\,K^{-1}$ at room temperature, which is similar to the corresponding result for the present glass, of $7.6 \times 10^{-6}\,K^{-1}$.

5.2. Composites

5.2.1. Theoretical models

A variety of theoretical models has appeared over the years, on the basis of which attempts have been made to explain the thermal expansion characteristics of composites in terms of the thermal expansion coefficients and elastic constants of the constituents. For convenience, the

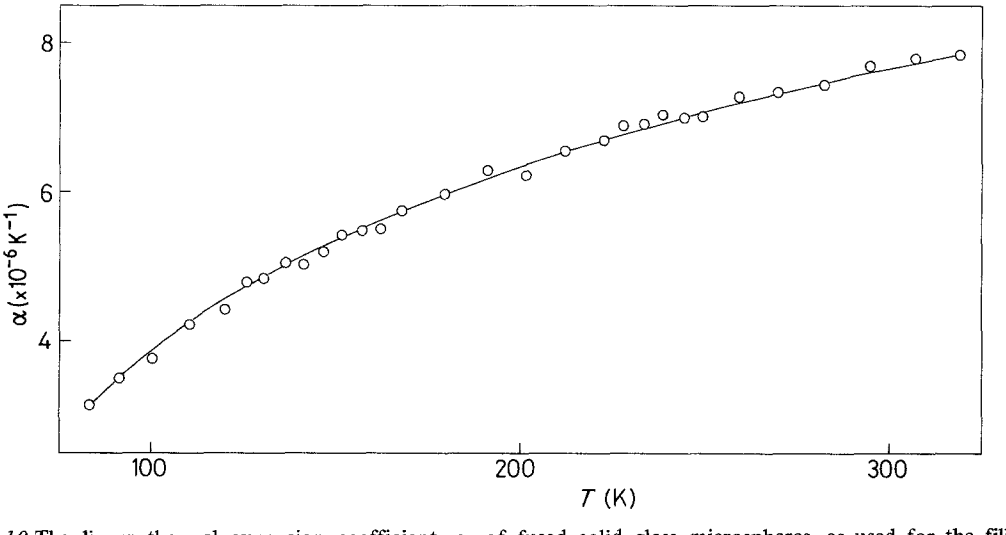

Figure 10 The linear thermal expansion coefficient, α, of fused solid glass microspheres, as used for the filler of Specimens 10 and 11.

symbols used in the following representative survey have been collected in the Nomenclature section at the start of the paper.

One of the earliest models, due to Turner [15], assumed that it was sufficiently realistic to regard each component as being surrounded by a homogeneous mixture, such that the sum of the internal forces might be equated to zero and that shear deformation might be neglected completely. On this basis the stress, S_i, on the ith component, resulting from a temperature rise, ΔT, might be written

$$S_i = (\beta_c - \beta_i)K_i \Delta T. \quad (3)$$

The argument required that the resultant of the forces on any cross-section of the mixture must be zero, and that the relative areas formed in the cross-section by the different components were proportional to their relative volumes. From these assumptions it followed that the volume coefficient of thermal expansion might be written as

$$\beta_c = \frac{(\beta_m K_m V_m) + (\beta_i K_i V_i)}{(K_m V_m) + (K_i V_i)}. \quad (4)$$

This model has enjoyed a great deal of success in accounting for the thermal-expansion characteristics of alloys.

In a later study, due to Kerner [16], the components were assumed to take the form of grains suspended in, and bonded to, some uniform bonding medium, the resulting composite being macroscopically isotropic and homogeneous. The grains were assumed to be distributed at random, and in order to be consistent with the idea of isotropy they were assumed to be spherical in shape. Some of the terms involved in the formulation of the equations were not explicitly defined in the contexts in which they were used, though there was one clear difference between the assumptions of Kerner [16] and Turner [15]. Kerner assumed the existence of an average shell of suspending medium surrounding an average grain, sufficiently far beyond which was the average medium, consisting of suspending medium and grains. When considering the equilibrium of the system, the ratio of the linear dimensions of an inclusion to those of the whole body was assumed to be equal to the ratio of the corresponding surface areas and volumes, and the case of tightly packed grains was considered by allowing the suspending medium to vanish. When this was done, expressions for the rigidities and bulk moduli emerged which involved properties of the vanished suspending medium. Evaluations of these moduli were made possible by supposing that in this limiting case these properties might be replaced by those of the average medium, an assumption which was mathematically consistent with the equations of Kerner. The resulting expression for the bulk modulus of the composite was given by solving

$$\sum \frac{K_i - K_c}{3K_i + 4n_c} = 0 \quad (5)$$

and

$$\sum \frac{(n_c - n_i)V_i}{(7 - 5\nu_c)n_c + (8 - 10\nu_c)n_i} = 0 \quad (6)$$

for K_c by eliminating n_c, after substituting for

$$\nu_c = f(K_c, n_c). \quad (7)$$

Extending his argument to include the effect of thermal stress, Kerner derived the following expression for the volume thermal expansion coefficient of the composite solid,

$$\beta_c = \left(\frac{4n_c}{K_c} + 3\right) \sum \frac{\beta_i K_i V_i}{4n_c + 3K_i}. \quad (8)$$

Employing a semi-empirical approach based upon the rule of mixtures, Thomas [17] derived the following expression for the linear thermal expansion coefficient of a composite, which took no account of the elastic properties of the constituents,

$$\beta_c = \beta_m^{V_m} \cdot \beta_i^{V_i}. \quad (9)$$

An alternative expression

$$\beta_c = \beta_m \left[1 - V_i \left(1 - \frac{\beta_i}{\beta_m}\right)\theta\right], \quad (10)$$

where

$$\theta = \frac{3(E_i/E_m)(1 - \nu_m)}{(E_i/E_m)[2V_i(1 - 2\nu_m) + (1 + \nu_m)] + 2(1 - 2\nu_i)(1 - V_i)}, \quad (11)$$

was deduced by Wang and Kwei [18]. Wang and Kwei regarded the filled matrix as a collection of spherical composites of various sizes, such that each spherical composite contained a filler particle and a concentric shell of matrix material. The authors applied appropriate boundary conditions to the solution of classical equations, in which account was taken of the positive or negative

interfacial mismatch of the thermally induced dimensional changes. Their result is the same as the later result of Fahmy and Ragai [19] and within 1% of results predicted by the earlier model of Schapery [20], when employing the lower bound of Hashin and Shtrikman [21] to calculate the bulk modulus of elasticity of the composite.

Yet another predictive equation was derived by Tummala and Friedberg [22], who regarded each dispersed particle as an elastic sphere embedded in an infinite elastic continuum, resulting in an axially symmetric stress distribution around the dispersion. The observed thermal expansion coefficient was regarded as the sum of the matrix thermal expansion coefficient modified by the effect of the dispersed phase upon the expansion of the matrix and the expansion coefficient of the dispersed phase modified by the effect of the matrix on the expansion of the dispersed phase. The expression finally derived was

$$\beta_c = \beta_m - V_i\phi(\beta_m - \beta_i), \quad (12)$$

where

$$\phi = \frac{(1+\nu_m)/2E_m}{[(1+\nu_m)/2E_m] + [(1-2\nu_i)/E_i]}. \quad (13)$$

A number of additional models have appeared over the years, but an appraisal of the present results will be limited to an examination of the applicability of the models mentioned.

5.2.2. Composites containing silica flour

5.2.2.1. Particle volume-fraction. The effect of inclusion volume-fraction upon the linear thermal expansion coefficient of the silica flour-containing composites is qualitatively obvious from Fig. 5, i.e., increasing the volume-fraction of the constituent having the lower thermal expansion coefficient lowered the thermal expansion coefficient of the resulting composite.

In order to be able to apply the models summarized earlier to the task of understanding these results in fundamental terms, a knowledge of the elastic constants of the resin and silica flour was required, as functions of temperature. The Young's modulus and Poisson's ratio of a specimen of resin were measured at the Railway Technical Centre, Derby, at room temperature, and found to be 3.38 GNm^{-2} and 0.39, respectively. The temperature dependence of the Young's modulus was estimated by supposing that this was similar to that of other epoxy resins for which the temperature dependence of the Young's modulus was known. In this assessment, use was made of the results of Pink and Campbell [23] for Araldite type MY753/HY951, Hartwig and Wüchner [24] for Ciba-Geigy resin CY221/HY979, Khayyat and Stanley [25] for Araldite type CT200/HT907 and Ledbetter and Maerz [26] for G-10CR and G-11CR. Data for the elastic constants of polycrystalline quartz were taken as averages of the Voigt and Reuss approximations from results given by Simmons and Wang [27] and values for the linear thermal expansion coefficient of silica were taken from an appraisal based upon a survey of the literature [28].

The extent to which the theoretical models correctly account for the influence of inclusion volume-fraction upon the linear thermal expansion coefficients of Specimens 1 to 4 is brought out in Fig. 11, in which smoothed experimental data at temperatures of 100 K, 200 K and 300 K are compared with the predictions of the different models. Curve 3 clearly provides the best fit and between the models to which it corresponds, that due to Wang and Kwei [18] is preferable to that of Schapery in that fewer input data are required to produce the final result. An alternative way of looking at these results is illustrated in Fig. 12, in which the influence of temperature is high-lighted in preference to inclusion volume-fraction. The conclusion regarding the superiority of the models corresponding to Curve 3 over the others is again apparent.

5.2.2.2. Particle size. It is clear from the results for Specimens 2, 5, 6 and 7, displayed in Fig. 6, that any influence of the size of the included particles, over the mean diameter range of 49 to 115 μm, at an inclusion volume-fraction of 20%, is beyond the detection limit of the apparatus over the approximate temperature range 85 K to 310 K. In a further search for particle-size effects the programme was extended to include composites containing particles which were available over a wider size range than the silica flour. One of these inclusions was chosen with a fairly high elastic modulus, i.e., glass in the form of solid microspheres; the other with a fairly low elastic modulus, i.e., copper in the form of powder.

5.2.3. Composites containing glass microspheres

Examination of Fig. 7 reveals no influence of a

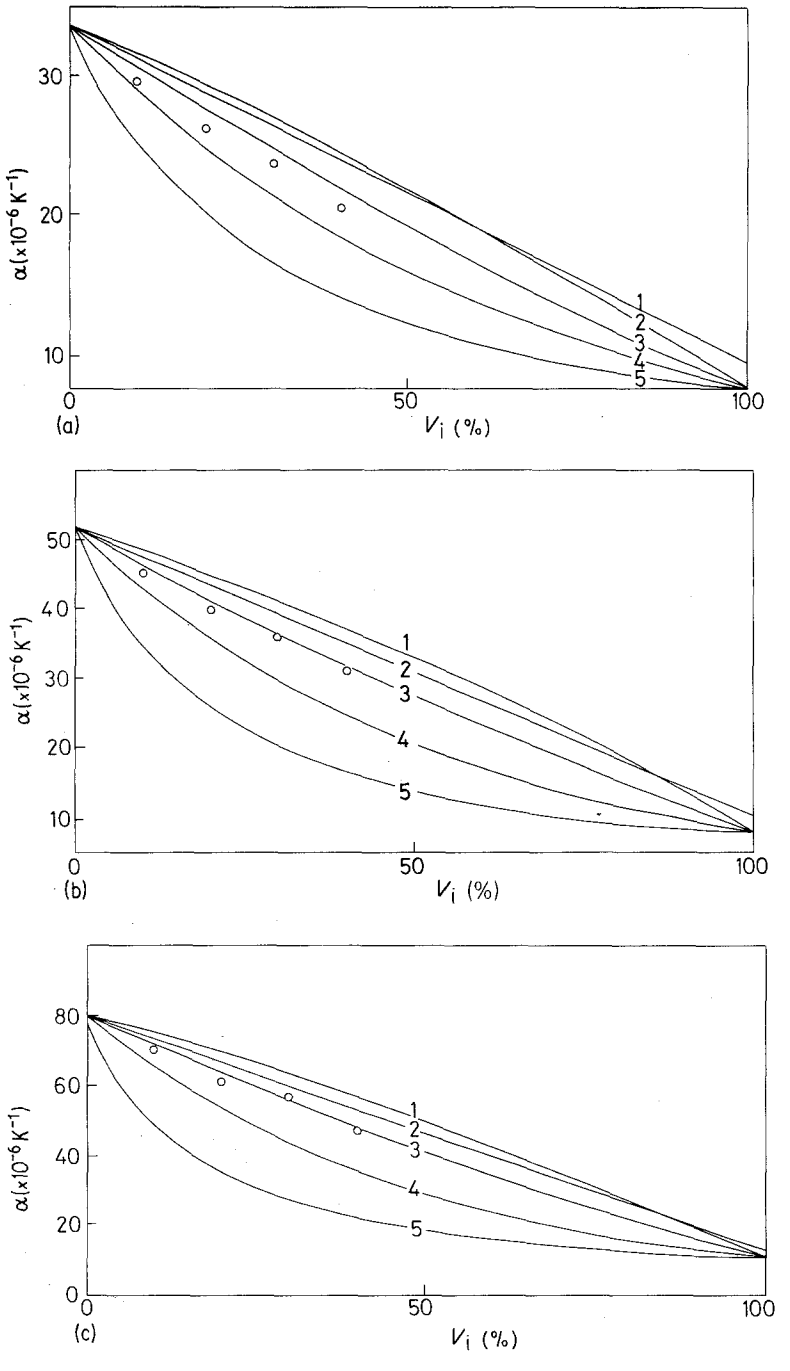

Figure 11 The experimentally determined influence of inclusion volume-fraction, V_i, upon the linear thermal expansion coefficient, α, of Ciba-Geigy epoxy resin, CY219/HY219/DY219, containing silica flour, compared with predicted values. (a) At 100 K, (b) at 200 K, (c) at 300 K: ○, smoothed experimental results for Specimens 1 to 4; Curve 1, Kerner [16]; Curve 2, Tummala and Friedberg [22]; Curve 3, Wang and Kwei [18]; Fahmy and Ragai [19] and Schapery [20]; Curve 4, Thomas [17] and Curve 5, Turner [15].

variation of the mean diameter of the microspheres over the range 22 to 237 μm, at a volume-fraction of 20%, upon the thermal expansion coefficient over the same temperature range as before. The applicability of the theoretical models mentioned earlier was again examined. In this evaluation the elastic constants were approximated at values for vitreous silica due to Fine *et al.* [29], extrapolated to room temperature. These were used together with measured values for the linear thermal expansion coefficient of fused glass microspheres, forming Specimen 9. The result (not shown) was the same as previously, i.e., the model of Wang and Kwei [18] and others producing essentially similar results accorded closest with the experimental data. The predominating influence of the resin in determining the thermal expansions of composites containing silica-flour or soda-lime glass

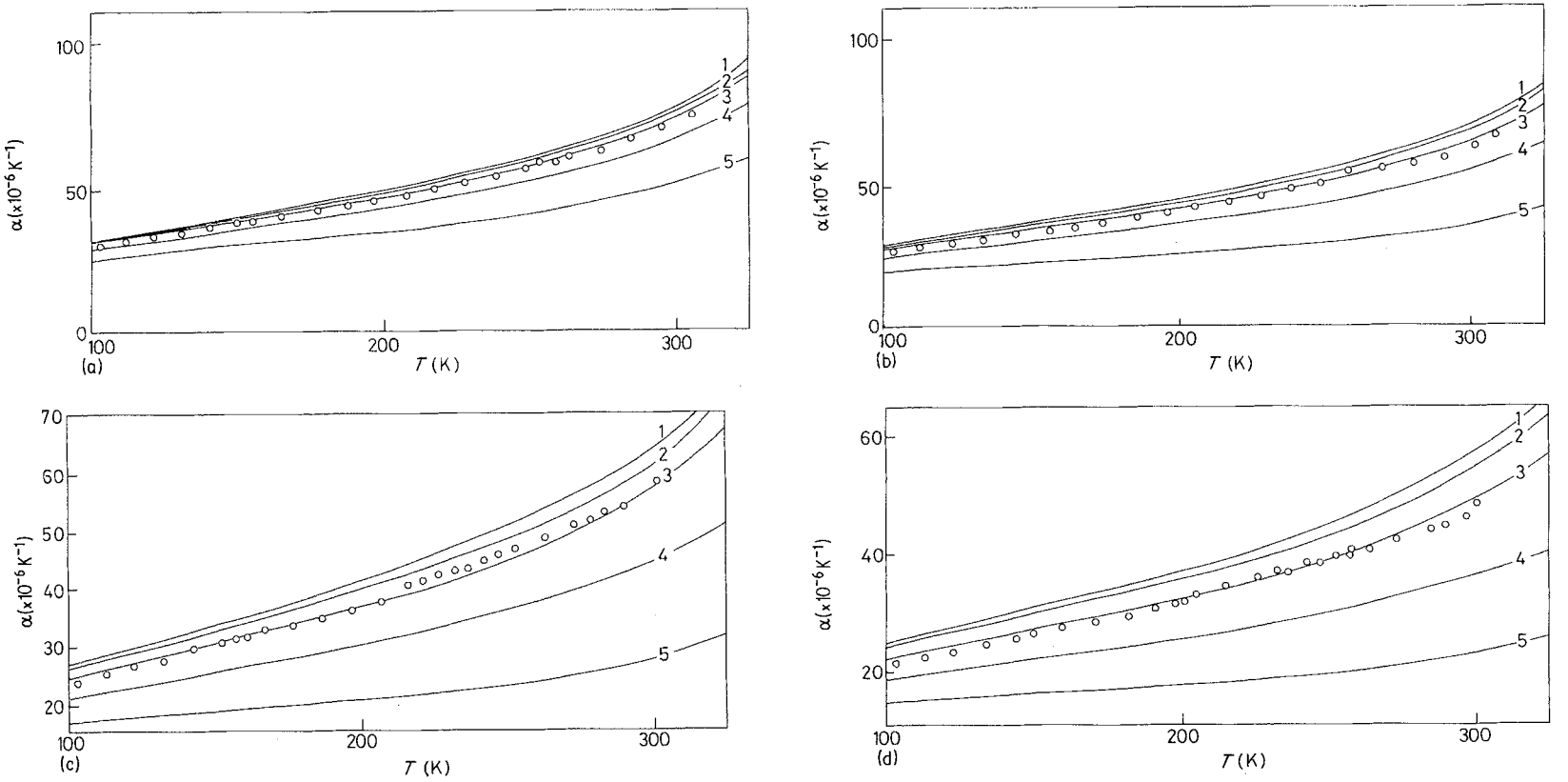

Figure 12 The experimentally determined influence of temperature upon the linear thermal expansion coefficient, α, of Ciba-Geigy epoxy resin, CY219/HY219/DY219, containing silica flour at different inclusion volume-fractions, V_i, compared with predicted values. (a) $V_i = 10\%$ (Specimen 1), (b) $V_i = 20\%$ (Specimen 2), (c) $V_i = 30\%$ (Specimen 3) and (d) $V_i = 40\%$ (Specimen 4); ○ primary experimental data; Curve 1, Kerner [16]; Curve 2, Tummala and Friedberg [22]; Curve 3, Wang and Kwei [18], Fahmy and Ragai [19] and Schapery [20]; Curve 4, Thomas [17]; and Curve 5, Turner [15].

microspheres at an inclusion volume-fraction of 20% is apparent from the similarity of the results for Specimens 2, 5, 6 and 7, as shown in Fig. 6, and Specimens 10 and 11, as shown in Fig. 7.

5.2.4. Composites containing copper powder

In common with observations of the absence of particle-size effects in the linear thermal expansion coefficient of resin-containing glass microspheres, Fig. 8 reveals no influence of particle-size effects in the case of reinforcement with copper powder. It is interesting to note, in passing, that the combined relative influences of the linear thermal expansion coefficients and elastic constants of glass and copper has been to produce lower thermal expansion coefficients in the composites reinforced with copper, as compared with composites containing glass microspheres, at nominally identical inclusion volume-fractions. In comparing observation with prediction the linear thermal expansion coefficients of copper given by Hahn [30] were employed, along with elastic constants given by Simmons and Wang [27]. Excluding the model of Thomas [17], which takes no account of elastic constants, the model agreeing best with observations (result not shown) was again that of Wang and Kwei [18].

6. Conclusions

Technological interest in the present work arose from a desire to be able to vary the thermal expansion characteristics of a loaded resin in a controlled manner, in order to be able to match this to the temperature-dependent dimensional changes of a body encapsulated by it. This has been achieved and it has been shown that the best quantitative representation of the results over a wide range of temperature was provided by the model of Wang and Kwei [18], and by later models producing identical or closely similar results.

Evidence of particle-size effects in the thermal properties of composites had been reported before the commencement of the present investigation and this provided one incentive for the search for such effects during the course of the present measurements. Droste and Dibenedetto [31] described an increase in the glass transition temperature, T_g, of a thermoplastic polymer amounting to several degrees, which resulted from increasing the concentration and specific surface area of the filler. Two fillers were used, Ballotini glass beads and Attapulgite clay. It was believed that polymer molecules were adsorbed on the surface of the filler particles. The resulting reduction of free volume was believed to have reduced molecular mobility and flexibility of the polymer chains in the vicinity of the interfaces which, in turn, raised the glass transition temperature. Support for this conclusion concerning the influence of particle-size effects on the glass transition temperature was provided by the later work of Pinheiro and Rosenberg [32], whose thermal expansion measurements indicated no influence from particle-size effects below T_g. Above this temperature a decrease of thermal expansion was found to result from reducing the particle size. An opposite effect has been reported by Filyanov [33], who observed a reduction in the glass transition temperature of an epoxy resin when this was loaded with glass microspheres. He explained this by supposing that a reaction between the surface of the filler particles and the resin had resulted in a reduction of the amount of hardener consumed in the curing process. This conclusion was strengthened by the enhanced water absorption of the loaded resin compared with that of the pure resin, which was associated with an excess of hardener resulting from the presence of the filler. Explanations of apparently conflicting observations such as these must be sought by analysing the detailed circumstances of each case individually. Thus, the absence of any noticeable particle-size effects in the present results does not rule out the possibility of their occurrence at a higher volume-fraction of filler or at a higher temperature than those employed in the present investigation.

Having identified a successful analytical scheme for predicting the thermal expansion behaviour of a particulate reinforced resin and, within limits, having established the relative unimportance of particle-size effects, one possible step forward is clear. In particular it should be possible to predetermine the thermal expansion–temperature relationship of a composite by selecting the matrix, filler and its loading according to their known thermal expansion and elastic modulus characteristics.

Acknowledgements

We wish to express our gratitude to Mr P. T. Wombwell for various forms of practical assistance, to Ciba-Geigy Plastics and Additives Company for their support of this project and to the Science

Research Council for a CASE award received by one of us (SJF). We also wish to thank Dr J. Batchelor and Mr P. J. Garrington, Railway Technical Centre, Derby, UK, for the Young's modulus and Poisson's ratio measurements of the resin specimen.

References

1. N. WATERHOUSE and B. YATES, *Cryogenics* **8** (1968) 267.
2. B. YATES, R. F. COOPER and M. M. KREITMAN, *Phys. Rev.* **B4** (1971) 1314.
3. C. HARWOOD, B. YATES and D. V. BADAMI, *J. Mater. Sci.* **14** (1979) 1126.
4. M. GLUYAS and C. HARWOOD, private communication (1977).
5. J. H. GLADSTON and J. DALE, *Phil. Trans.* **148** (1858) 887.
6. R. K. KIRBY and T. A. HAHN, Data sheet for NBS SRM 739, May 1971 (National Bureau of Standards, Washington, DC, USA).
7. K. F. ROGERS, L. N. PHILLIPS, D. M. KINGSTON-LEE, B. YATES, M. J. OVERY, J. P. SARGENT and B. A. McCALLA, *J. Mater. Sci.* **12** (1977) 718.
8. B. YATES, M. J. OVERY, J. P. SARGENT, B. A. McCALLA, D. M. KINGSTON-LEE, L. N. PHILLIPS and K. F. ROGERS, *ibid.* **13** (1978) 433.
9. B. YATES, B. A. McCALLA, J. P. SARGENT, K. F. ROGERS, L. N. PHILLIPS and D. M. KINGSTON-LEE, *ibid.* **13** (1978) 2217.
10. H. T. SMYTH, *J. Amer. Ceram. Soc.* **38** (1955) 140.
11. T. H. K. BARRON, *Ann. Phys.* **1** (1957) 77.
12. M. BLACKMAN, *Phil. Mag.* **3** (1958) 831.
13. A. J. LEADBETTER, *Phys. Chem. Glasses* **9** (1968) 1.
14. G. K. WHITE, *Cryogenics* **4** (1964) 2.
15. P. S. TURNER, *J. Res. Nat. Bur. Stand.* **37** (1946) 239.
16. E. H. KERNER, *Proc. Phys. Soc.* **B69** (1956) 808.
17. J. P. THOMAS, "Effect of Inorganic Fillers on Coefficient of Thermal Expansion of Polymeric Materials", Publication number AD 287-826, Contract number AF33(657)-7248, Armed Services Technical Information Agency, USA.
18. T. T. WANG and T. K. KWEI, *J. Polymer Sci.* **7** (1969) 889.
19. A. A. FAHMY and A. N. RAGAI, *J. Appl. Phys.* **41** (1970) 5108.
20. R. A. SCHAPERY, *J. Comp. Mater.* **2** (1968) 380.
21. Z. HASHIN and S. SHTRIKMAN, *J. Mech. Phys. Solids* **11** (1963) 127.
22. R. R. TUMMALA and A. L. FRIEDBERG, *J. Appl. Phys.* **41** (1970) 5104.
23. E. PINK and J. D. CAMPBELL, *J. Mater. Sci.* **9** (1974) 658.
24. G. HARTWIG and F. WÜCHNER, *Rev. Sci. Instrum.* **46** (1975) 481.
25. F. A. KHAYYAT and P. STANLEY, *J. Phys. D* **11** (1978) 1237.
26. H. M. LEDBETTER and G. MAERZ, *Cryogenics* **11** (1980) 655.
27. G. SIMMONS and H. WANG, "Single Crystal Elastic Constants and Calculated Aggregate Properties: a Handbook" (MIT Press, Cambridge, Mass., 1971) pp. 178–182.
28. Y. S. TOULOUKIAN, R. K. KIRBY, R. E. TAYLOR and T. Y. R. LEE, "Thermophysical Properties of Matter: Thermal Expansion, Non-metallic Solids" Vol. 13 (IFI/Plenum Press, New York, 1977) p. 350.
29. M. E. FINE, H. VAN DUYNE and N. T. KENNEY, *J. Appl. Phys.* **25** (1954) 402.
30. T. A. HAHN, *ibid.* **41** (1970) 5096.
31. D. H. DROSTE and A. T. DIBENEDETTO, *J. Appl. Polymer Sci.* **13** (1969) 2149.
32. M. DE F. F. PINHEIRO and H. M. ROSENBERG, *J. Polymer Sci. Polymer Phys. Ed.* **18** (1980) 217.
33. Ye. M. FILYANOV, *Polymer Sci. USSR* **20** (1979) 2074.

Received 27 November
and accepted 15 December 1981